



Fermi National Accelerator Laboratory

FERMILAB-Conf-93/206-E
CDF

The Center-of-Mass Angular Distribution of Prompt Photons Produced in $p\bar{p}$ Collisions at $\sqrt{s} = 1.8$ TeV

The CDF Collaboration

*Fermi National Accelerator Laboratory
P.O. Box 500, Batavia, Illinois 60510*

August 1993

Submitted to the *International Symposium on Lepton and Photon Interactions*,
Cornell University, Ithaca, New York, August 10-15, 1993



Disclaimer

This report was prepared as an account of work sponsored by an agency of the United States Government. Neither the United States Government nor any agency thereof, nor any of their employees, makes any warranty, express or implied, or assumes any legal liability or responsibility for the accuracy, completeness, or usefulness of any information, apparatus, product, or process disclosed, or represents that its use would not infringe privately owned rights. Reference herein to any specific commercial product, process, or service by trade name, trademark, manufacturer, or otherwise, does not necessarily constitute or imply its endorsement, recommendation, or favoring by the United States Government or any agency thereof. The views and opinions of authors expressed herein do not necessarily state or reflect those of the United States Government or any agency thereof.

The Center-of-Mass Angular Distribution of Prompt Photons Produced in $p\bar{p}$ Collisions at $\sqrt{s} = 1.8$ TeV

The CDF Collaboration

Abstract

Data taken with the Collider Detector at Fermilab (CDF) during the 1992-1993 run of the Tevatron are used to measure the distribution of the center-of-mass angle between isolated prompt photons and the beam direction. The shape of the angular distribution for photon-jet events is found to differ from the predictions of NLO QCD.

Submitted International Symposium on Lepton and Photon Interactions,
Cornell University, Ithaca, NY, August 10-15, 1993

Prompt photons produced in $p\bar{p}$ collisions provide good quantitative tests of perturbative Quantum Chromodynamics (QCD). Previous publications from UA2 [1] [2] and CDF [3] have shown good agreement between data and the predicted prompt photon cross section over a wide range of photon and center-of-mass (CM) energies. Perturbative QCD predicts that the CM angular distribution of prompt photon events will differ significantly from that of dijet events. This was demonstrated with data taken during the earlier 1988-1989 run [4]. Leading order (LO) prompt photon production, at Tevatron energies, is dominated by the t-channel quark exchange process ($gq \rightarrow q\gamma$); here the spin $\frac{1}{2}$ quark propagator produces a photon angular distribution roughly of the form $(1 - \cos \theta^*)^{-1}$, where θ^* is the CM polar angle. In contrast, dijet production is dominated by the t-channel gluon exchange process ($gg \rightarrow gg$), where the spin 1 gluon produces a jet angular distribution roughly of the form $(1 - \cos \theta^*)^{-2}$. At next-to-leading order (NLO), there are also diagrams (photon bremsstrahlung) contributing to the prompt photon process which have t-channel gluon exchange. Here we report early results from a partial data set from the 1992-93 run corresponding to an integrated luminosity of 5 pb^{-1} .

The data satisfied a trigger requiring an isolated electromagnetic cluster with a minimum transverse energy ($E_T = E \sin \theta = P_T$ for photons) of 16 GeV in the Central Electromagnetic Calorimeter [5]. The candidate events were reconstructed and energy corrections were applied to the electromagnetic (EM) and jet clusters [5] [6]. Additional requirements were imposed to ensure that photons were well measured. These include a cut on the pseudorapidity of the photon ($|\eta_\gamma| < 0.9$), a maximum displacement along z of the event vertex from the center of the detector ($|z_{\text{vert}}| < 50 \text{ cm}$) and fiducial cuts to avoid dead regions of the detector. Stringent isolation requirements were placed upon the photon candidates. The photon candidate cluster was required to have a second highest energy cluster in the Central Strip Chambers with Energy $< 1.0 \text{ GeV}$ and have less than 2.0 GeV unclustered EM E_T (CEM) within a cone radius $R=0.7$, centered about the photon, where $R=\sqrt{\Delta\phi^2 + \Delta\eta^2}$.

The stringent isolation cuts and a veto on any tracks pointing to the calorimeter tower of the photon candidate reduce the possible prompt photon backgrounds from events where a QCD jet fragments into a single isolated neutral meson that decays into *multiple* photons. The background subtraction method exploits the average difference in shower profiles expected from events with single isolated prompt photons and those with multiple photons originating from decaying neutral mesons. The shower profiles in both ϕ and z views are compared to a sample profile obtained from test beam electrons and a χ^2 is extracted for each view on an event by event basis. The average (χ_{ave}^2) of the two views is then used for the background subtraction [5] which obtains a weight for each event to be signal or background. The sum of the weights for signal and background is unity. The final signal/background mix is roughly 65% signal and 35% background. Of roughly 200,000 photon candidates in this data sample (5 pb^{-1}), roughly 10,000 pass all photon quality and $\cos \theta^*$ (Table 1) cuts.

In an effort to retain the simplicity of the $2 \rightarrow 2$ system, we vectorially sum the momentum from jets opposite to the photon, in ϕ , to create a single ‘summed’ jet. We require that the highest P_T jet be in the opposite hemisphere in ϕ from the photon and that the jet P_T be $> 10 \text{ GeV}/c$ after all energy corrections. We then add in second or third jets if they are also in the opposite hemisphere and have a corrected $P_T > 10 \text{ GeV}/c$. The CM variables are found from the P_T and direction of the photon candidate and the direction of the summed jet.

Var	Region 1	Region 2
$\pm \cos \theta^*$	0.0 to ± 0.6	± 0.3 to ± 0.8
$\pm \eta^*$	0.0 to ± 0.7	± 0.3 to ± 1.1
η_{Boost}	∓ 0.9 to ± 0.2	∓ 1.2 to ∓ 0.2
p^*	20.1 to 45.0 GeV/c	26.7 to 47.0 GeV/c

Table 1: Table of cuts on the CM variables that ensure uniform acceptance for $\cos \theta^*$.

The angular distribution presented is $\frac{d^2N}{dp^*d\cos\theta^*}$, where we have integrated over a range of the CM momentum p^* . Since there can be no angular asymmetry in this measurement, we plot vs. $|\cos \theta^*|$. In the case of a $2 \rightarrow 2$ system, the CM variables p^* , η^* and η_{Boost} can be found from the P_T of the photon, and the detector pseudorapidities of the photon and the jet ($\eta_\gamma, \eta_{\text{Jet}}$) via: $\eta^* = \frac{\eta_\gamma - \eta_{\text{Jet}}}{2}$, $\eta_{\text{Boost}} = \frac{\eta_\gamma + \eta_{\text{Jet}}}{2}$, $p^* = P_T \cosh \eta^*$ and $\cos \theta^* = \tanh \eta^*$.

In order to utilize as much of the data as possible, we select two regions (see Table 1), each uniform in η^* and η_{Boost} acceptance, and normalize in a region of overlap. The boxes in Fig. 1 define the regions of uniform acceptance in η^* and η_{Boost} . The corresponding cuts for $\cos \theta^*$ are given in Table 1. The p^* limits for uniform acceptance are the result of the combined limits on P_T ($16 < P_T < 45$ GeV/c) and η^* (explicitly, $p_{\text{min}}^* = p_{T\text{min}} \cdot \cosh \eta_{\text{max}}^*$ and $p_{\text{max}}^* = p_{T\text{max}} \cdot \cosh \eta_{\text{min}}^*$). Fig. 2 plots P_T vs. η^* and illustrates this effect on the transformation to p^* . The lines are curves of constant P^* . The minimum P^* accepted is determined by the point where the minimum P_T ($=16$ GeV) touches the highest η^* of a region. The largest systematic uncertainty of the measurement comes from the statistics of the overlap region and therefore an increase in momentum range is vital to the measurement. In the latest experimental run of CDF the lowest unrescaled photon trigger threshold was lowered from 23 to 16 GeV which greatly aided in increasing the momentum range over the 88-89 data.

Fig. 3 shows the prompt photon $\cos \theta^*$ distribution after background subtraction plotted against predictions from a full NLO [8] calculation of prompt photon production. Also shown are a LO calculation [9] of dijet production and the background data, subtracted from the data and normalized in the same fashion as the signal. The theory curves and data have a normalization such that the flat part of the curve $|\cos \theta^*| < 0.3$ has an area of 0.3. The inner error bars of Fig. 3 show the statistical uncertainties only, the outer are the statistical and systematic uncertainties added in quadrature. The theory curves were generated at the parton level and were required to pass the same isolation requirements as the data. The prompt photon data do not agree well with NLO theory, however the background data agree very well with LO dijet theory (and dijet data). The source of background are jet events with rare fragmentation of a jet into a single high P_T neutral meson, decaying to photons, so the agreement with dijet theory is expected. In the NLO calculations the outgoing partons were summed and the resultant direction was used to calculate $\cos \theta^*$, in the same fashion as the data.

The systematic uncertainties include effects from the normalization, uncertainties in the χ^2 distributions for background subtraction, trigger efficiency and acceptance [7]. The normalization uncertainty was estimated with the 1σ statistical variation within the regions used for normalization. There is an overall normalization, completely correlated, common to all eight points ($\sim 4\%$) and a relative normalization uncertainty between the last two

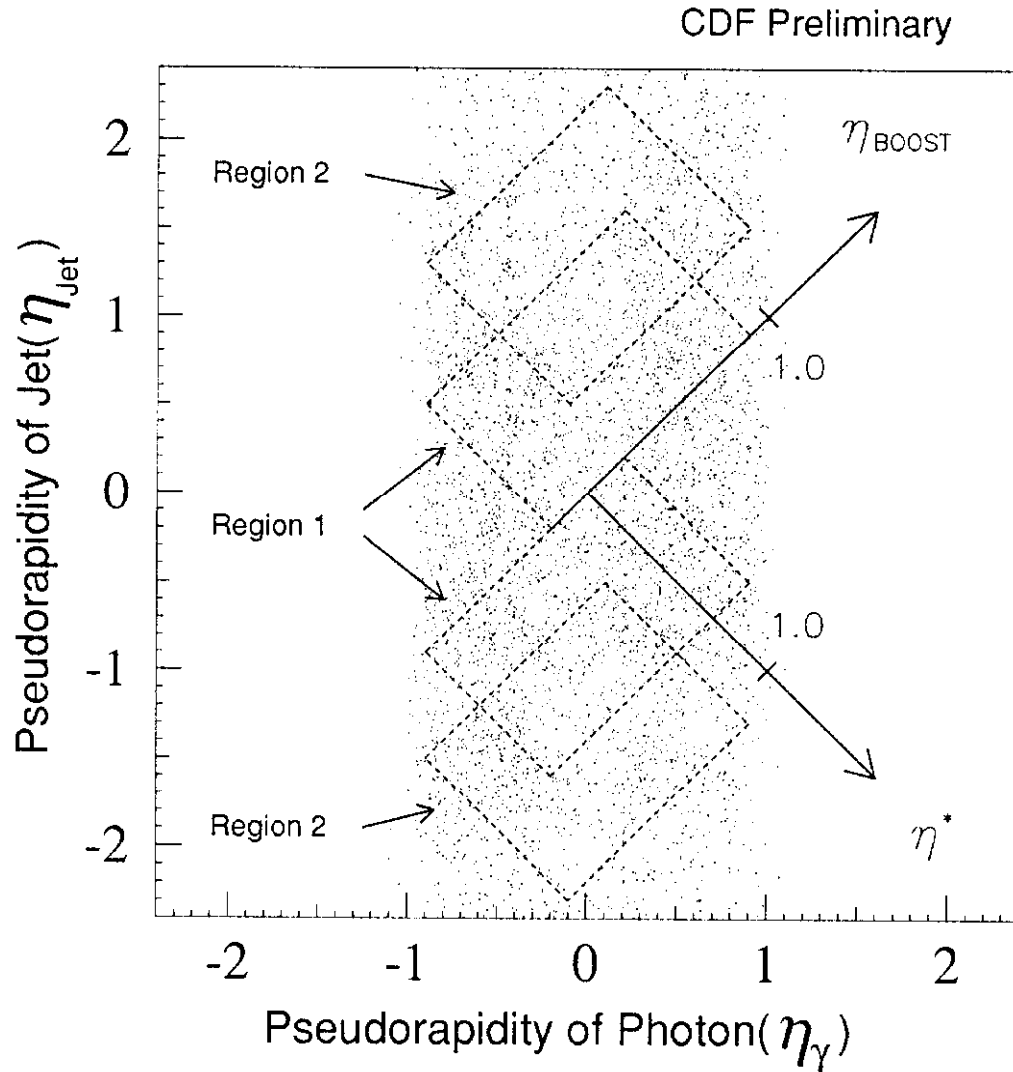


Figure 1: Data plotted η_{Jet} vs. η_γ . The diagonal axes are the sum (η_{Boost}) and difference (η^*) axes. The overlapping regions are used for normalization.

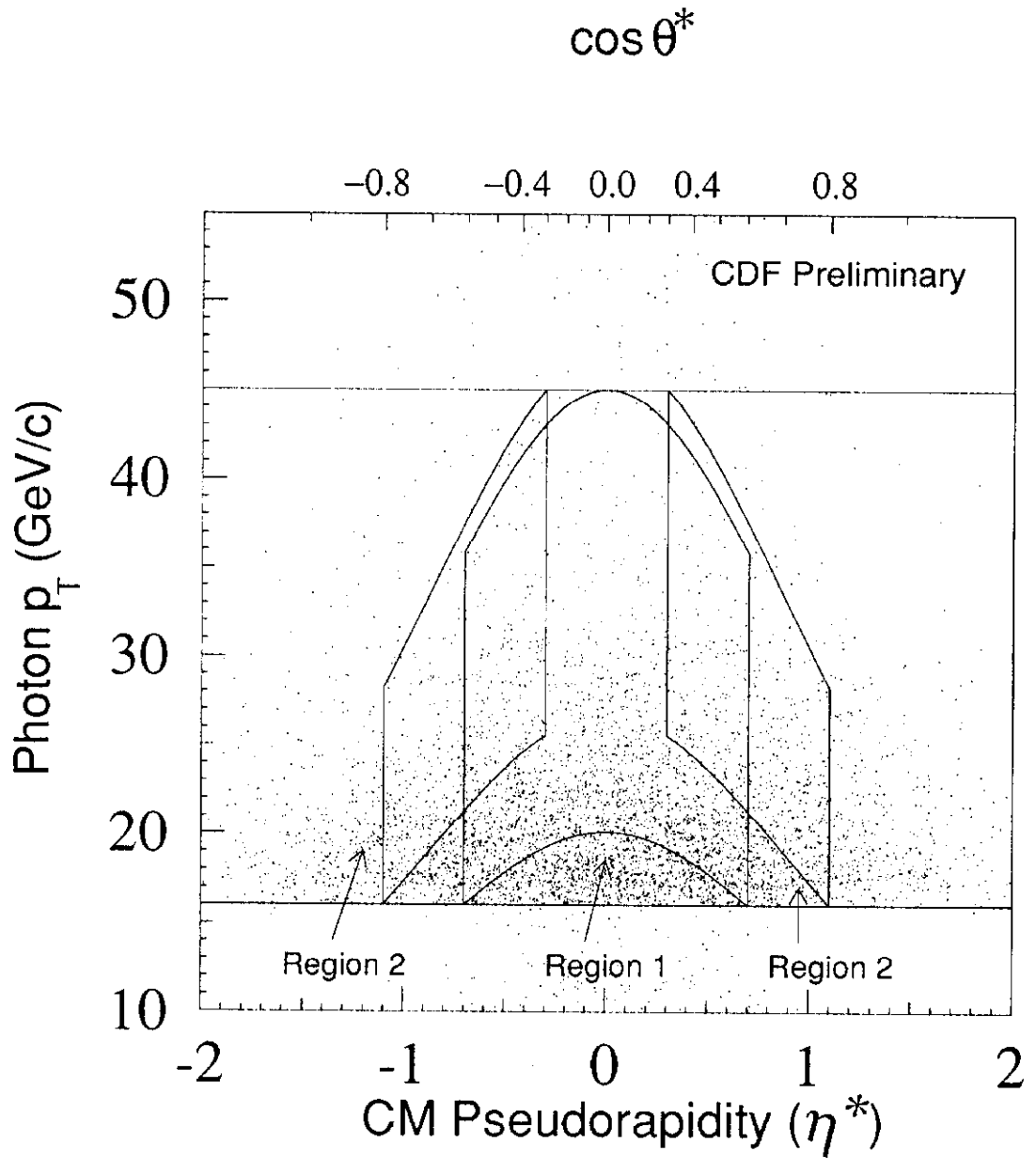


Figure 2: Data plotted P_T vs. η^* . The vertical lines delineate the regions in η^* ($\cosh \theta^*$) and the curves are contours of constant p^* . The points within the curves are regions of flat acceptance in p^* and η^* . The horizontal lines are the upper and lower limits of $p_{T\min} = 16$ GeV/c and $p_{T\max} = 45$ GeV/c which along with the limits on η^* correspond to $20.1 < p^* < 45.0$ GeV/c and $26.7 < p^* < 47.0$ GeV/c in each of the uniform acceptance regions. The $\cos \theta^*$ scale is given along the upper axis for reference.

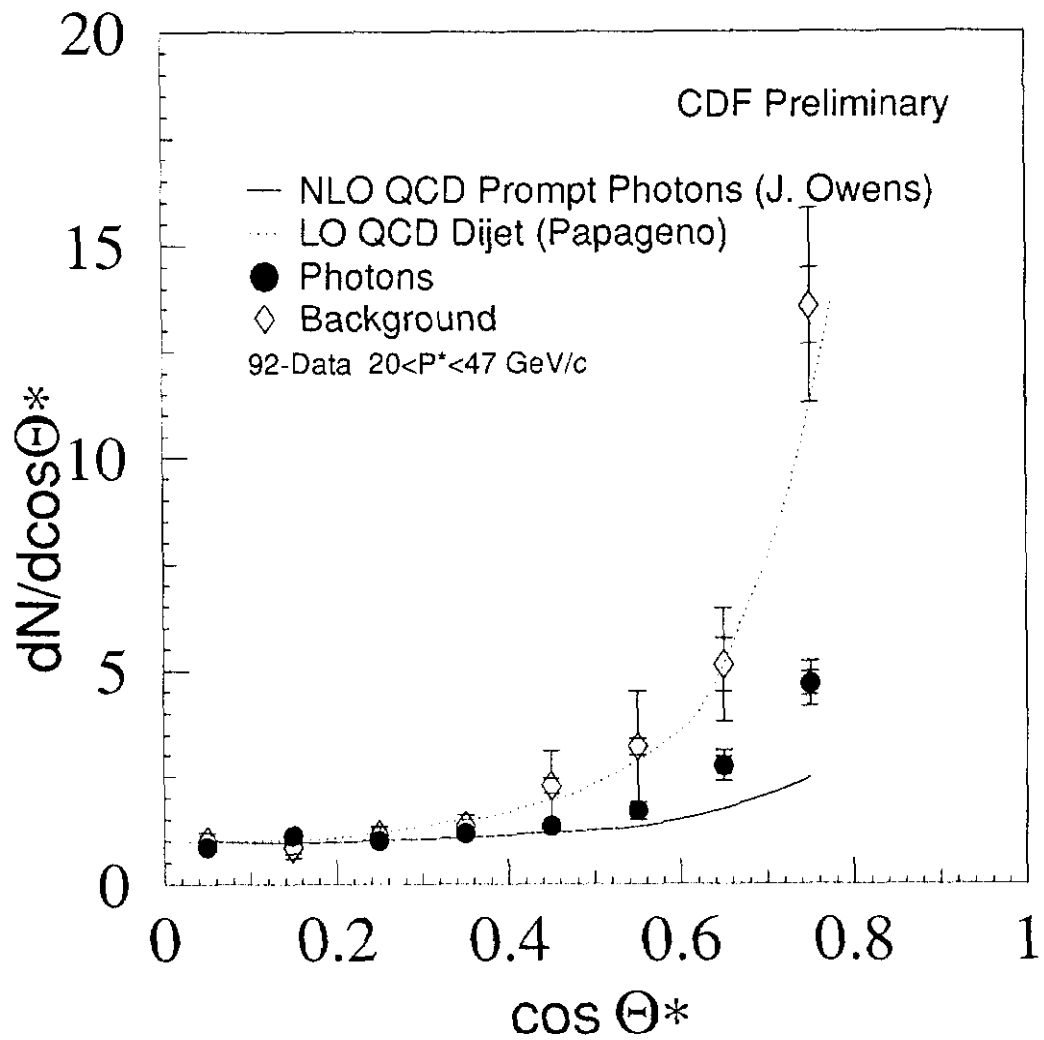


Figure 3: Direct Photon $\cos \theta^*$ Signal and Background for the SumJet method for the 92-93 data. Inner error bars are statistical errors only, the outer are statistical and systematic errors added in quadrature.

points and the other six ($\sim 6.3\%$). The uncertainties on the angular distribution due to the background subtraction and trigger efficiency uncertainty were found by repeating the analysis with the simulation χ_{ave}^2 distributions and trigger efficiency varied independently by their 1σ uncertainties. Both uncertainties get larger with increasing $\cos\theta^*$ reaching a maximum of 3.8% and 2% respectively. The systematic uncertainties from η^* and η_{Boost} acceptance were found from a Monte Carlo detector simulation to be $< 5\%$ [7].

In Fig. 4 we plot the same angular distribution but forming the angle $\cos\theta^*$ from only the Photon and the lead jet (in P_T) rather than the vector sum of all jets in the hemisphere opposite the photon as before. A quick comparison of Figs. 3 and 4 will convince the reader that both methods give the same result.

The discrepancy between the data and NLO QCD could be due to an insufficient contribution from the bremsstrahlung diagram in the NLO calculation. Higher order calculations might alleviate this problem. Photons originating from a bremsstrahlung process in general should have associated jet activity from the quark line closest to the photon. While presumably many such events would fail the CDF isolation cuts, the jet topology of the events that do pass provides information about the production mechanism. Events selected with jets near the photon should be preferentially photons originating from bremsstrahlung processes. In the above $\cos\theta^*$ plots we have already demanded that the lead jet be in the hemisphere opposite to the photon in ϕ , so to test our hypothesis we divide the data sample into those events that have *additional* jet activity in the same hemisphere in ϕ and those that do not. Identifying jets at relatively low P_T is difficult, so to be conservative we plot in Fig 5. a) events with 2nd or 3rd jets with $P_T > 10$ GeV in the same hemisphere in ϕ as the photon and b) those with no 2nd or 3rd jets with $P_T > 5$ GeV on the same side. The relative samples represent a) 20% (additional same side jets) and b) 50% (no same jets) of the data shown in Figs. 3 and 4. As can be seen in Fig. 5 the angular distribution of the data tends to steepen (more like the background) when there are jets in the same hemisphere and flatten out (closer to NLO QCD theory) when no additional same side radiation is present. This would support the idea that the bremsstrahlung process is a source of the discrepancy between the data and NLO QCD theory. The increased importance of this process was already hinted at in the inclusive photon cross-section previously published by CDF [3] and these data support this idea.

The authors wish to thank the technical and support staffs of Fermilab and the participating institutions. We would also like to thank H. Baer, J. Ohnemus and J.F. Owens for use of the results of their theoretical calculations. This work was supported by the U.S. Department of Energy, the National Science Foundation, the Italiano Istituto Nazionale di Fisica Nucleare, the Ministry of Science, Culture and Education of Japan, the Natural Sciences and the Alfred P. Sloan Foundation.

References

- [1] UA2 Collaboration, J. Alitti *et al*, Phys. Lett. B **263**, 544 (1991).
- [2] UA2 Collaboration, J. Alitti *et al*, Phys. Lett. B **288**, 386 (1992).
- [3] F. Abe *et al*, Phys. Rev. Lett. **68**, 2734 (1992).

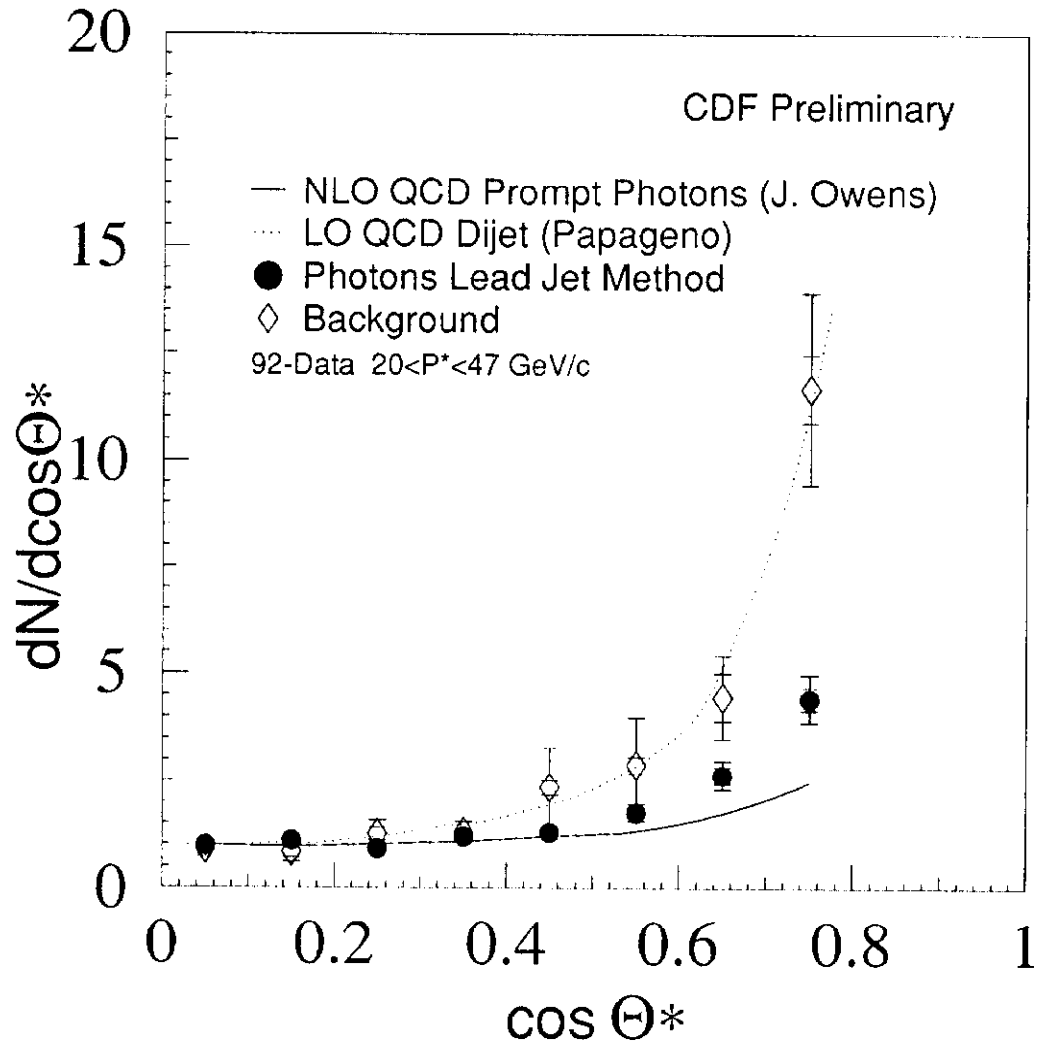


Figure 4: Direct Photon $\cos \theta^*$ Signal and Background for the LeadJet method for the 92-93 data. Inner error bars are statistical errors only, the outer are statistical and systematic errors added in quadrature.

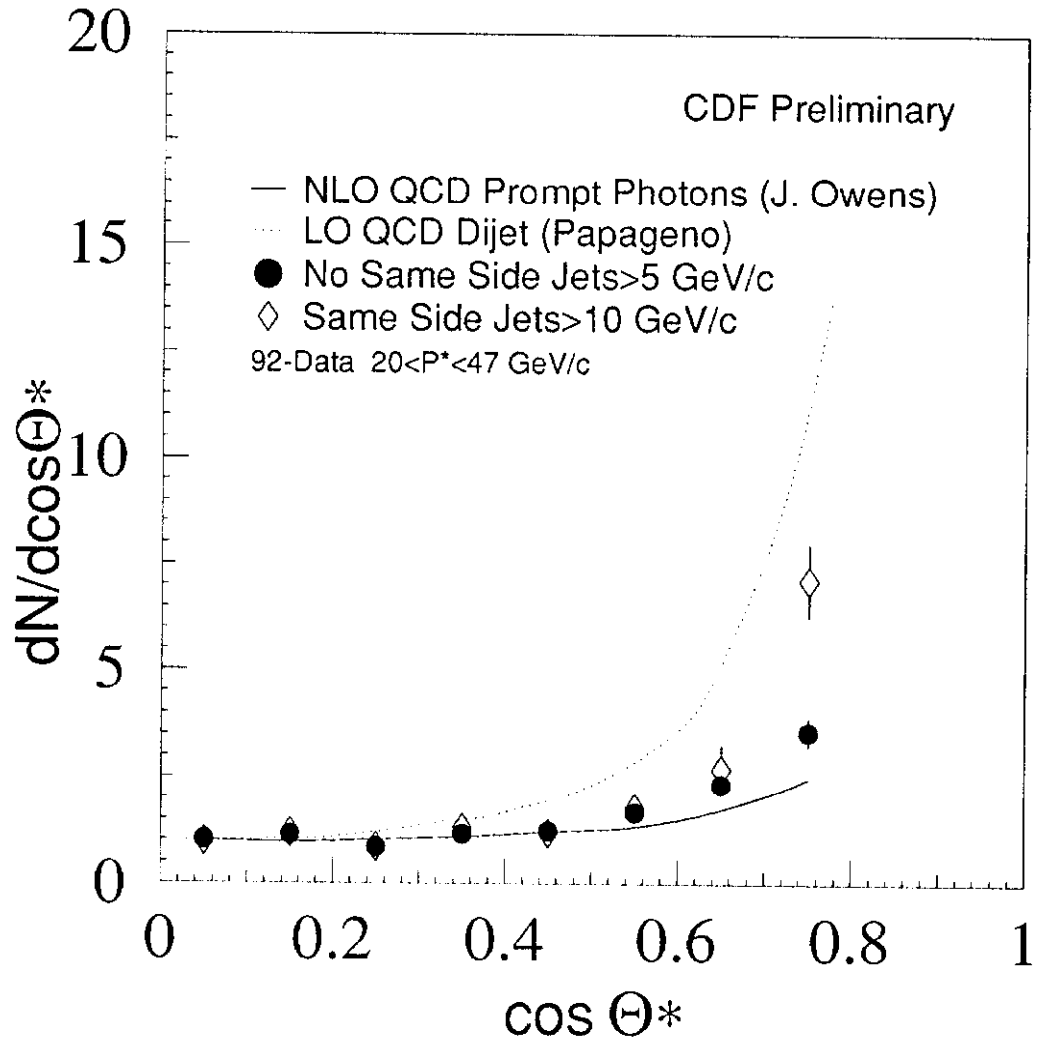


Figure 5: Direct Photon $\cos \theta^*$. Signal cut with same side and no same side jets. 'Same side jets' has a 2nd and/or 3rd Jet with $P_T > 10$ GeV/c in the same hemisphere in ϕ as photon candidate. 'No same side jets' has no 2nd or 3rd Jet with $P_T < 5$ GeV/c in the same hemisphere as the photon. Statistical errors only.

- [4] F. Abe *et al*, Fermilab-PUB-93/032-E, 1993 (to be published in Phys. Rev. Lett.).
- [5] F. Abe *et al*, Fermilab-PUB-92/01-E, 1992 (to be published in Phys. Rev. D.).
- [6] F. Abe *et al*, Phys. Rev. Lett. **68**, 1104 (1992).
- [7] L. Nakae, Ph.D. thesis, Brandeis University, April 1992.
- [8] H. Baer, J. Ohnemus and J.F. Owens, Phys. Lett. **234B**, 127 (1990).
- [9] I Hinchcliffe, *Papageno* Event Generator, Private Communication.